REPORT DOCUMENTATION PAGE

Form Approved
OMB No. 0704-0188

PLEASE DO NOT RETURN YOUR FORM TO THE ABOVE ADDRESS.

1. REPORT DATE *(DD-MM-YYYY)*	2. REPORT TYPE	3. DATES COVERED *(From - To)*
04/08/2008	Final Performance Technical Report	October 1, 2003-September 30, 2006

4. TITLE AND SUBTITLE

Analysis of Vorticity and Turbulence Measurements in a Wake of a Bridge Pier

5a. CONTRACT NUMBER

5b. GRANT NUMBER

N00014-03-1-0967

5c. PROGRAM ELEMENT NUMBER

6. AUTHOR(S)

Thomas B. Sanford

5d. PROJECT NUMBER

5e. TASK NUMBER

5f. WORK UNIT NUMBER

7. PERFORMING ORGANIZATION NAME(S) AND ADDRESS(ES)

Applied Physics Laboratory, University of Washington
1013 N.E. 40th Street
Seattle, WA 98105

8. PERFORMING ORGANIZATION REPORT NUMBER

9. SPONSORING/MONITORING AGENCY NAME(S) AND ADDRESS(ES)

Thomas Swean
Office of Naval Research
875 North Randolph Street
Arlington, VA 22203-195

10. SPONSOR/MONITOR'S ACRONYM(S)

11. SPONSOR/MONITOR'S REPORT NUMBER(S)

12. DISTRIBUTION/AVAILABILITY STATEMENT

UU

13. SUPPLEMENTARY NOTES

14. ABSTRACT

Dissipation rates of turbulence kinetic energy and enstrophy are reported in a high Reynolds number turbulent wake. Our results represent a set of rare field observations of vorticity and turbulence in a turbulent wake with a high Reynolds number. The turbulent wake was formed by an unsteady strong tidal current interacting with a bridge pier. Measurements were taken in the intermediate wake. Both energy and enstrophy show a similar downstream decay rate faster than that predicted by the self-preservation similarity in the far wake. The theoretical relation for high Reynolds number flow is confirmed by field observations. The magnitudes of the vertical and horizontal components of enstrophy are not significantly different. Probability density functions of normalized vorticity components and of the dissipation rate of turbulence kinetic energy are nearly identical to each other. They are also nearly identical to the empirical function found in laboratory experiments. The turbulence internal intermittency is ~0.2, estimated from autocorrelation coefficients of enstrophy; this value is close to that reported previously in turbulent wakes and jets.

15. SUBJECT TERMS

16. SECURITY CLASSIFICATION OF:			17. LIMITATION OF ABSTRACT	18. NUMBER OF PAGES	19a. NAME OF RESPONSIBLE PERSON
a. REPORT	b. ABSTRACT	c. THIS PAGE			Thomas B. Sanford
UU	UU	UU	UU	1	19b. TELEPHONE NUMBER *(Include area code)* 206-543-1365

Submitted to IEEE Journal of
Engineering, January 2008

Vorticity and Turbulence in the Wake of a Bridge Pier

R.-C. Lien and T. B. Sanford

Received: ; Revised:

R.-C. Lien and T.B. Sanford, Applied Physics Laboratory, University of Washington, Seattle, WA 98105, USA. (lien@apl.washington.edu and sanford@apl.wasington.edu)

DOI:

Keywords: Vorticity, Turbulence, Wake, Vibration

ABSTRACT

Dissipation rates of turbulence kinetic energy ε and enstrophy ζ^2 are reported in a high Reynolds number turbulent wake. Previous turbulent wake observations have been made in laboratory experiments with relatively low Reynolds number flows, $O(10^3)$. Our results represent a set of rare field observations of vorticity and turbulence in a turbulent wake with a high Reynolds number, $O(10^7)$. The turbulent wake was formed by an unsteady strong tidal current interacting with a bridge pier. Measurements were taken in the intermediate wake. Both ε and ζ^2 show a similar downstream decay rate faster than that predicted by the self-preservation similarity in the far wake. The theoretical relation $\varepsilon = \nu\zeta^2$ for high Reynolds number flow is confirmed by field observations. The magnitudes of the vertical and horizontal components of enstrophy are not significantly different. Probability density functions of normalized vorticity components and of the dissipation rate of turbulence kinetic energy are nearly identical to each other. They are also nearly identical to the empirical function found in laboratory experiments. The turbulence internal intermittency is ~0.2, estimated from autocorrelation coefficients of enstrophy; this value is close to that reported previously in turbulent wakes and jets.

1. INTRODUCTION

Turbulent wakes have been studied extensively in laboratory experiments, numerical models, and theoretical studies. Field observations of turbulent wakes are difficult to obtain because the natural environment is not controllable, the spatial scale is too large to cover synoptically, and the turbulent wake is often unsteady. Natural turbulent wakes often have a Reynolds number $Re_d = u_\infty d \upsilon^{-1}$, where u_∞ is the free-stream velocity, d the scale of the obstacle, and υ the kinematic molecular viscosity, many decades greater than those laboratory and numerical experiments can achieve. Whether results obtained in the relatively low Reynolds number flows are applicable to high Reynolds number natural flows remains a question.

In turbulent wakes vorticity plays the most important dynamic role. The vorticity is generated via the flow field interacting with the obstacle and cascades to larger scales. Unfortunately, vorticity is a difficult variable to obtain because it requires accurate measurements of velocity gradients. In laboratory experiments Antonia et al. [1] designed a probe to measure vorticity in the wake of a circular cylinder with a Reynolds number $O(10^3)$. Sanford et al. [2] presented the first set of oceanic vorticity measurements in a tidal channel with a Reynolds number $O(10^7)$, using a unique electro-magnetic vorticity meter (EMVM) that also measures velocity and dissipation rate of turbulence kinetic energy ε.

Here, we present observations of vorticity ζ and turbulence kinetic energy dissipation rate ε in a turbulent wake behind the pier of the Tacoma Narrows Bridge in Washington State, with $Re_d > 2 \times 10^7$. The turbulent wake was established by a strong, unsteady, decelerating tidal current in the presence of a weak cross-wake shear.

The experiment and measurements are described in section 2. General statistics of vorticity and turbulence kinetic energy dissipation rates are presented in section 3. The downstream variation of ε and self-preservation properties are discussed in section 4. The downstream variation of enstrophy ζ^2 and turbulence intermittency determined from their autocorrelation coefficients are described in section 5, and a summary follows in section 6.

2. Experimental Conditions

A. Instruments and Measurements

Measurements of velocity, vorticity, and turbulence kinetic energy dissipation rates were taken behind a pier of the Tacoma Narrows Bridge (Fig. 1a) during a brief study in southern Puget Sound. Within 3 h, three sets of zigzag-transect observations were taken downstream from the pier during the decelerating phase of the northward ebb tidal current. Tidal currents in Tacoma Narrows often exceed 2 m s^{-1}. An aerial photo of the old Tacoma Narrows Bridge, taken >50 years ago soon after its failure, reveals vortices generated behind the pier (Fig. 1b). Similar vortices and turbulence formed in the wake of the new Tacoma Narrows Bridge pier are the focus of this analysis.

Our primary instrument is the EMVM tow body (Fig. 1c). Sensors on the EMVM include two EM velocity and vorticity meters (VMs), a microstructure shear probe, and a CTD sensor. Details of sensors and measurements are described in Table 1. The principle of measuring vorticity and velocity using the VM, and sensor response functions are described by Sanford et al. [2].

One VM is mounted on the bottom of the EMVM (Fig. 1c; labeled EM velocity and vorticity sensor). It measures the streamwise (i.e., along the axis of the EMVM) and the spanwise (transverse to the axis of the EMVM) components of velocity and the vertical component of vorticity. Another VM is mounted on the side of the EMVM. It measures the streamwise and the vertical components of velocity, and the spanwise component of vorticity. Measurements of ε are obtained from the microstructure shear probe in front of the EMVM. Ancillary sensors measure the pitch, compass, pitch rate, and yaw rate. These ancillary measurements are needed to remove the instrument motion from velocity and vorticity measurements.

Because of the finite size of the vorticity sensor, variations of vorticity and velocity at scales smaller than the sensor separation, 0.09 m, are attenuated in VM measurements [2]. The turbulence velocity has red spectral characteristics, i.e., large eddies contain most of the energy. Turbulence velocity measurements are less affected by the sensor attenuation at small scales. The turbulence vorticity has a blue spectrum. Most of the enstrophy is at scales close to the Kolmogorov scale, $\eta = \upsilon^{3/4}\varepsilon^{-1/4}$. Because the Kolmogorov scale decreases with increasing turbulence intensity, the amount of sensor

attenuation on our vorticity measurements increases with turbulence intensity. Sanford et al. [2] derive response functions of the sensor attenuation for velocity and vorticity. They demonstrate that the sensor attenuation effect can be corrected. In the following analysis, response functions of the vorticity and velocity are applied to our measurements to correct for the missing variances at small scales.

The EMVM was towed at speeds of 1–2 m s^{-1} through the water at a depth of ~5.5 m in water of 15–40 m depth (Fig. 1a). Measurements were taken from upstream of the pier to 2–3 km downstream of the pier. The pier is located in water of ~40 m depth and has a nearly square shape of ~30 m on each side (d = 30 m). Most previous wake studies have focused on turbulent wakes behind a cylinder.

In this analysis we rotate the coordinate system into the along-wake and across-wake components (Fig. 1a). The along-wake coordinate is defined as 61 degrees counterclockwise from east, and the across-wake coordinate is 90 degrees counterclockwise from the along-wake coordinate. Similarly, measured horizontal velocity is rotated to the along-wake and across-wake components.

B. Free-stream Velocity

Our measurements were taken for ~3 h beginning from the peak of an ebb tidal current. To obtain the estimates of the free-stream velocity u_∞, we compute averages of the streamwise velocity taken during the zigzag transects outside of the wake (Fig. 2). The free-stream velocity decreased from 2.5 m s^{-1} to 0.5 m s^{-1} within 3 h and exhibited a slight

transverse gradient, likely due to the lateral boundary friction. We fit the observed free-stream velocity to a model consisting of a constant transverse gradient, a mean current, and a semidiurnal tidal current described as

$$u_\infty^m(y,t) = [1 - y\partial_y u_\infty][\bar{u} + u_t \cos(\omega t)], \quad (1)$$

where $\partial_y u_\infty = 6.3 \times 10^{-4}$ s^{-1} is the fitted transverse gradient of the free-stream velocity, $\bar{u}$ = 1.09 m s^{-1} is the fitted mean current, u_t = 1.32 m s^{-1} is the fitted tidal current amplitude, and $\omega = 2\pi/12.4$ h is the lunar semidiurnal frequency. The model-fit free-stream velocity u_∞^m is used to estimate the turbulence kinetic energy dissipation rate predicted by the turbulent wake self-preservation similarity and to compare with our direct observations of turbulence kinetic energy dissipation rate. During the three lateral transects, the ship was set downstream by the tidal flow at average speeds of 1.95, 1.87, and 1.01 m s^{-1}, respectively. The average free-stream velocity during the three transects was 2.2, 1.9, and 1.0 m s^{-1} through the water (similar to the ship's drift velocity). The average free-stream velocity is used to scale observed dissipation rates of turbulence kinetic energy and enstrophy in sections 4 and 5.

3. Statistics of Enstrophy and Turbulence Kinetic Energy Dissipation Rate

In high Reynolds number flow, the dissipation rate of turbulence kinetic energy is related to the turbulent enstrophy as[3]

$$\varepsilon = \upsilon \zeta^2 \quad (2)$$

where ζ^2 is the total enstrophy, i.e., the sum of the squares of the three components of vorticity. This relation has been justified in low Reynolds number, $Re = 1530$, flows in lab experiments [4]. Our measurements were taken in the field flow with $Re_d > 2 \times 10^7$, given $u_\infty > 1$ m s^{-1}, $d = 30$ m, and $\upsilon = 1.4 \times 10^{-6}$ m^2 s^{-1}. Therefore, we expect (2) to be satisfied.

Only one of the two components of horizontal vorticity was measured. We assume that the vorticity field is horizontally homogeneous and estimate the total enstrophy as $\zeta^2 = 2\zeta_h^2 + \zeta_z^2$, where ζ_h^2 is the spanwise enstrophy and ζ_z^2 is the vertical enstrophy. Large-scale coherent vortices in the turbulent wakes might not be homogeneous. However, they have weaker enstrophy. Most of the vorticity variance is at small scales, characteristic of blue spectra. Therefore, the horizontal homogeneity assumption should be satisfied approximately.

We computed the average spanwise and vertical components of enstrophy in each transect when the ship steamed at a nearly constant velocity, excluding measurements when the ship turned, accelerated, or decelerated. The horizontal and vertical components of enstrophy have a similar magnitude and are significantly correlated with a correlation coefficient of 0.8 and the 95% significance level of 0.35 (Fig. 3a). At an intermediate enstrophy strenght, the vertical component is slightly greater than the horizontal component. The estimates of total enstrophy agree with observed ε (Fig. 3b), as suggested by the high Reynolds number relation. The correlation coefficient between the logarithms of ζ^2 and ε is 0.91, with the 95% significance level of 0.35.

The probability density functions (pdf) of the magnitudes of vorticity components and the total vorticity, and the pdf of $\varepsilon^{1/2}$ have an exponential form [4], i.e.,

$$p(\lambda) \sim \exp(-\beta\lambda/\sigma_\lambda), \tag{3}$$

with $\beta = 1.4$, where λ represents any of demeaned $|\zeta_z|$, $|\zeta_h|$, $|\zeta|$, and $\varepsilon^{1/2}$, and σ_λ represents the standard deviation of λ. The pdfs of observed ε and vorticity magnitudes show a nearly identical exponential form (Fig. 2c). They closely follow the empirical formula (3). These results (Fig. 3) confirm the quality of measurements of ζ and ε, and form the basis of the following analysis. Furthermore, the close agreement concludes that the empirical pdf formula derived from low Reynolds number flows exists also in the high Reynolds number field flows.

4. Downstream Variations in Turbulence Kinetic Energy Dissipation Rates

A. Observed Turbulence Kinetic Energy Dissipation Rates Along the Centerline

We compute ε in 1-s intervals and examine its downstream variation. Because of the limited spatial resolution of our measurements to resolve the cross-wake and along-wake structure and to avoid the complexity of the cross-wake variation, we only investigate the downstream variation of the dissipation rates along the centerline of the wake. The Tacoma Narrows bends at ~1800 m downstream from the pier of the Tacoma Narrows Bridge (Fig. 1a) beyond which the modulation of vorticity and turbulence by the lateral boundary cannot be ignored. In the following analysis, we discuss only observations within 1800 m downstream of the pier.

Turbulence kinetic energy dissipation rates ε observed within 10 m from the centerline of the wake are averaged, typically a 10-s time interval with the ship's drift velocity of ~4 kts (Fig. 4). Upstream of the pier the background turbulence is not weak, ε ~10^{-5} W kg^{-1}, showing the turbulent nature of the flow in Tacoma Narrows. Such an energetic background is different from most laboratory experiments in which a weak turbulence background is often enforced.

During the first two legs of the experiment, there were no observations at the wake's centerline within 400 m downstream of the pier. At ~400 m downstream from the pier, ε is 20–50 times of that observed upstream of the pier. Further downstream, it decays almost monotonically with distance. The observed ε has a similar magnitude during the first two legs, and is the weakest in the third leg, as expected in the weakening ebb tidal current.

The third transect shows a weak value of ε at 300 m downstream and the strongest ε at 800 m downstream. Our measurements do not have sufficient spatial and temporal resolutions to investigate this departure from the expected monotonic downstream decay. The turbulence intermittency and unsteadiness of the turbulent wake might be the sources for the observed discrepancy.

The dependence on the tidal forcing is better illustrated by the normalized ε and the normalized downstream distance, scaled respectively as $\varepsilon_* = \varepsilon/(u_\infty^3 d^{-1})$ and $x_* = x/d$ (Fig.

4b). The choice of normalization is discussed in the next section. This normalization reduces the nearly one-decade scattering of ε to within a factor of two (Figs. 4a and 4b).

We apply two types of curve fittings, power law and exponential, to observations within $12 < x_* < 60$ to yield $0.01(x_* / x_c)^{-3}$ and $0.008e^{-(x_* - x_c)/10}$. The referenced downstream scale $x_c = 12$ is chosen where the observed ε is the strongest. The dimensionless amplitude, 0.01 and 0.008, the power law x_*^{-3}, and the exponential decay scale 10 d are parameters determined by the least squared fit to observations. The obtained –3 power law is steeper than that predicted by the self-preservation similarity in the turbulent far wake, as reviewed in the next two sections. Sreenivasan [5] reports that the decay rate of a temperature anomaly in a heated cylindrical turbulent wake is faster in the intermediate and near wake than in the far wake. Our observed x_*^{-3} decay rate for ε in the intermediate wake does not conflict with results of previous studies.

B. Review of Self-preservation Similarity in a High Reynolds Number Turbulent Far Wake

In a turbulent wake, mean and turbulence properties may be expressed as functions of two parameters [3], the velocity defect at the centerline of the wake, $u_s = u_\infty - u(y = 0)$, where $u(y=0)$ is the along-wake velocity at the centerline, and ℓ, the half-wake thickness defined as $u_s / 2 = u_\infty - u(y = \lambda)$. Both ℓ and u_s vary in the downstream direction (x-component) and depend on the obstacle scale d and the free-stream velocity u_∞ expressed as [6]

$$\lambda = C_\lambda d \left(\frac{x - x_0}{d}\right)^{1/2} \tag{4}$$

$$u_s = C_u u_\infty \left(\frac{d}{x - x_0}\right)^{1/2}, \tag{5}$$

where x_0 is the virtual origin. Previous studies report indefinite values of the virtual origin, varying from –40 *d* to –125 *d*. Some argue that the virtual origin depends on the Reynolds number. The values of coefficients C_λ and C_u are estimated as 0.2 and 1.28 by Browne and Antonia [6]. Similar values are reported elsewhere [3].

The along-wake and across-wake self-preservation similarity of velocity, the dissipation rates of turbulence kinetic energy, and enstrophy are described as [3]

$$\frac{u_\infty - \bar{u}}{u_s} = f_u(y_*) \tag{6}$$

$$\varepsilon = \frac{u_s^3}{\lambda} f_\varepsilon(y_*) = C_\varepsilon \left[u_\infty^3 / d\right] d/(x - x_0)\Big]^2 f_\varepsilon(y_*) \tag{7}$$

$$\zeta^2 = \frac{u_s^3}{\nu\lambda} f_\varepsilon(y_*) = C_\varepsilon \left[u_\infty^3 / \nu d\right] d/(x - x_0)\Big]^2 f_\varepsilon(y_*), \tag{8}$$

where $y_* = y\lambda^{-1}$ is the non-dimensional cross-wake coordinate, and $C_\varepsilon = C_u^3 / C_\lambda$.

The analytical form for the cross-wake structure $f_u(y_*)$ and $f_\varepsilon(y_*)$ have been discussed previously [7, 8, 9]. This is beyond the scope of our study and will not be discussed further.

Previous experiments conclude that the self-preservation properties establish at x > 100 *d* in the far wake [10, 11]. Our observations are taken at x < 60 *d*, in the near and intermediate wake regions and the observed turbulent wake is unsteady due to the time varying tidal current. We do not expect self-preservation similarity to apply to our

observations. Nonetheless, we construct a pure kinematic model on the basis of the self-preservation similarity and compare model results with observations, not to justify the similarity scaling, but to emphasize the difference.

C. Model Prediction of ε

Following the steady-state self-preservation similarity, we construct a similarity scaling imposed by a time varying free-stream velocity as

$$\varepsilon_m(x,y,t) = g(u_s(x,t),\lambda(x,t))f_\varepsilon(y_*), \tag{8}$$

where ε_m is the model dissipation rate, g is a function of time varying velocity scale $u_s(x,t)$ and the wake scale $\lambda(x,t)$. We assume that $u_s(x,t)$ and $\lambda(x,t)$ scale by the time varying free-stream velocity $u_\infty^m(t)$, and the obstacle scale d. The proposed scaling for ε is described as

$$\varepsilon_m(x,t) = \left\{C_\varepsilon u_\infty^3(t_0)d^{-1}\right\}\left\{d^2\left[\int_{t_0}^{t} u_\infty^m(t')dt' - x_0\right]^{-2}\right\}f_\varepsilon(y_*) = H_\varepsilon(x,t)f_\varepsilon(y_*). \tag{9}$$

The downstream distance from the pier is $x = \int_{t_0}^{t} u_\infty^m(t')dt'$, where t_0 is the time when the turbulence is generated at the pier. Turbulence is advected downstream by the decaying tidal current.

Turbulence kinetic energy dissipation rate predicted by the above equation for $x_0 = -40d$ is shown in Fig. 5. The model results of ε at the centerline are compared with our observations (Fig. 4). Model results decrease by nearly one decade during the 3-h

experiment period, similar to the range of observed variation (Fig. 4a), and have a magnitude comparable to our observations. However, the downstream variation of ε_m is much slower than the observed x^{-3} variation. Model ε_m varies as x^{-2} in the far field, $x \gg x_0$, far beyond our observation regime. Model results using different virtual origins reveal the similar slower downstream decay rate than the observed x^{-3} decay rate.

The observed x^{-3} cannot be explained by the time varying free-stream velocity. We propose that x^{-3} is the true decay rate of dissipation rates of turbulence kinetic energy in the intermediate wake. The faster decay rate of turbulence is further confirmed by the variation of the observed turbulence enstrophy.

5. Enstrophy Properties

A. Observations of Enstrophy Along Centerline

The downstream variations of the vertical and horizontal components of enstrophy along the centerline of the turbulent wake, within 10 m, are shown in Figs. 6 and 7. The background value of both components of enstrophy, upstream from the pier, is about 1 s^{-2}. At ~300 m downstream from the pier, both components of enstrophy increase by more than two decades above the upstream intensity. They decrease downstream nearly monotonically and by more than one decade at 1600 m from the pier. Both components of enstrophy during leg 2 are stronger than those during leg 3, as expected by the tidal forcing. Unexpectedly, both components of enstrophy during leg 1 are weaker than those during leg 2. We do not have an explanation but attribute this to turbulence randomness.

We normalize the observed enstrophy by $u_\infty^3 / d\upsilon$, in accordance to the scaling for ε. This normalization does not collapse the scattering significantly, partially due to the unexpected low enstrophy during leg 1. The power law fit yields $\propto x_*^{-2.4}$ and $\propto x_*^{-2.7}$ for the vertical and the horizontal components of enstrophy, respectively, in close agreement with the downstream decay rate of ε. The exponential fit yields the decaying scale of ~10 d, again consistent with that of ε.

B. Turbulence Intermittency

The spatial spottiness of the fine scale structure, the so-called internal intermittency, is a well-known feature of turbulence. Previous studies often quantify the intermittency using the decay rate of the autocorrelation of turbulence properties with increasing lags. Shafi et al. [12] investigate the intermittency within a turbulent wake using the structure of the autocorrelation of enstrophy, i.e.,

$$\gamma_{\zeta^2}(R) = \langle \zeta^2(r)\zeta^2(r+R)\rangle / \sigma_{\zeta^2}^2 \sim (L/R)^{\mu}, \tag{10}$$

where the exponent μ is the intermittency, R is the spatial lag, and L is the turbulence integral length scale. Previous studies report the intermittency μ to be about 0.2 in low Reynolds number flows [12, 13].

We compute the autocorrelation coefficients using observed enstrophy within 10 m from the centerline and within 10 and 60 d downstream from the bridge pier. Observations taken at irregular spatial intervals are first interpolated to a constant spatial interval ~ 0.1 m

before computing the autocorrelation coefficients γ_{ζ^2}. Values of γ_{ζ^2}, averaged within prescribed intervals of spatial lags, of both enstrophy components exhibit a monotonic decaying power exponent close to those reported previously [12]. During our experiment, ε varies between 10^{-6} and 10^{-3} W kg^{-1}, and η varies from 0.03 cm to 0.1 cm. The autocorrelation coefficient decreases at a nearly constant rate for lags between 0.3 m and 4 m, corresponding to $300 < R/\eta < 10^4$. We interpret this as being part of the turbulence inertial subrange. Outside of this range, the autocorrelation coefficient exhibits different slopes with respect to the spatial lags. The power exponent decay rates, i.e., the intermittency μ for $\gamma_{\zeta_z^2}$ and $\gamma_{\zeta_h^2}$ within 0.3–4-m scales, are 0.2 and 0.22, respectively, computed by fitting logarithmic values of γ_{ζ^2} and R using the least squared method. These results are in near agreement to those reported in previous studies of turbulent wakes and jets [12].

6. SUMMARY

Dissipation rates of turbulence kinetic energy and the vertical and horizontal components of enstrophy were measured in a turbulent wake behind a bridge pier. The turbulent wake is generated by the tidal current. Our observations confirm the relation between the enstrophy and dissipation rates of turbulence kinetic energy in high Reynolds number flows, and confirm the empirical probability density functions reported in previous laboratory studies.

Dissipation rates of turbulence kinetic energy and two components of enstrophy near the centerline exhibit a similar downstream decay rate, one faster than that predicted by the self-preservation similarity in the far wake. We propose that the larger decay rate exists in the intermediate wake.

The turbulence intermittency is estimated using the autocorrelation function of the two components of enstrophy. Autocorrelation coefficients of enstrophy exhibit distinct slopes in different ranges of spatial lags. In the scale much greater than the Kolmogorov length scale and smaller than 4 m, identified as a part of the inertial subrange, the intermittency is close to 0.2, consistent with laboratory experimental results.

ACKNOWLEDGMENTS

This work is supported by the Office of Naval Research. The authors thank J. Riley of the University of Washington and I. Afanassiev of the Memorial University of Newfoundland for helpful discussions and J. Dunlap, J. Carlson, and E. Boget (all APL-UW) for their help during the experiment.

REFERENCES

[1] R. A. Antonia, D. A. Shah, and L. W. B. Browne, "Dissipation and vorticity spectra in a turbulent wake," *Phys. Fluids*, vol. 31, p. 6, 1988.

[2] T. B. Sanford, J. A. Carlson, J. H. Dunlap, M. D. Prater, and R.-C. Lien, "An electro-magnetic vorticity and velocity sensor for observing finescale kinetic fluctuations in the ocean," *J. Atmos. Ocean. Technol.*, vol. 16, pp. 1647–1667, 1999.

[3] H. Tennekes, and J. Lumley, *A First Course in Turbulence*. Cambridge, MA: MIT Press, 1972.

[4] Y. Zhu, and R. A. Antonia, "On the correlation between enstrophy and energy dissipation rate in a turbulent wake," *Appl. Sci. Res.*, vol. 57, pp. 337–347, 1997.

[5] K. R. Sreenivasan, "Evolution of the centerline probability density function of temperature in a plane turbulent wake," *Phys. Fluids*, vol. 24, pp. 1232–1234, 1981.

[6] L. W. B. Browne and R. A. Antonia, "Reynolds shear stress and heat flux measurements in a cylinder wake," *Phys. Fluids*, vol. 29, pp. 709–713, 1986.

[7] A. A. Towsend, *The Structure of Turbulent Shear Flow*. Cambridge University Press, 1956.

[8] I. Wygnanski, F. Champagne, and B. Marasli, "On the large-scale structures in two-dimensional, small-deficit, turbulent wakes," *J. Fluid Mech.*, vol. 168, pp. 31–71, 1986.

[9] X. Liu, F. O. Thomas, and R. C. Nelson, "An experimental investigation of the planar turbulent wake in constant pressure gradient," *Phys. Fluids*, vol. 14, pp. 2817–2838, 2002.

[10] R. A. Antonia and J. Mi, "Approach towards self-preservation of turbulent cylinder and screen wakes," *Exp. Therm. Fluid Sci.*, vol. 17, pp. 227–284, 1998.

[11] P. Freymuth and M. Uberoi, "Structure of temperature fluctuations in the turbulent wake behind a heated cylinder," *Phys. Fluids*, vol. 14, pp. 2574–2580, 1971.

[12] H. S. Shafi, Y. Zhu, and R. A. Antonia, "Intermittency of vorticity in a turbulent shear flow," *Phys. Fluids*, vol. 8, pp. 2245–2247, 1996.

[13] K. R. Sreenivasan and P. Kailasnath, "An update on the intermittency exponent in turbulence," *Phys. Fluids A*, vol. 5, pp. 512–514, 1993.

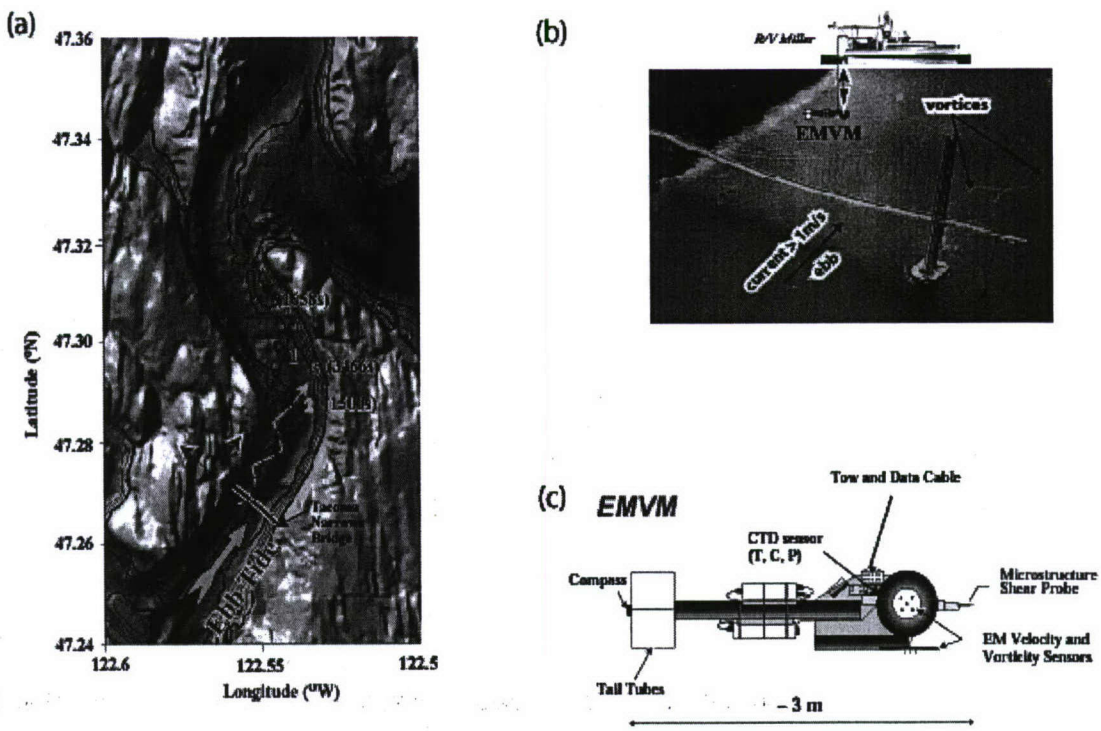

FIG. 1. (a) Bathymetry of Tacoma Narrows and ship tracks. Land is shades of gray; water bathymetry is all other colors colors. Thin contours are 10-m isobaths; the thick black contour is 50 m depth. The red, yellow, and magenta zigzag curves are ship tracks during the first, second, and third surveys (as labeled), respectively, downstream of a pier of the Tacoma Narrows Bridge (shown as a black line with white edges). Values inside parentheses indicate the total sampling period in seconds. The thick yellow arrow illustrates the direction of the ebb tide. The two perpendicular red arrows indicate the coordinate system in the downstream and cross stream directions. (b) Photograph of vortices behind the pier of the Tacoma Narrows Bridge taken soon after the bridge collapsed in 1940. (c) Sketch of Electro-Magnetic Vorticity Meter (EMVM). Two vorticity meters (VMs) are mounted on the side and the bottom, respectively. A microstructure shear probe is mounted in the front of the EMVM. CTD sensors and a pressure sensor are mounted on the side of the EMVM. Other measurements include compass, pitch, pitch rate, and yaw rate of the EMVM to calibrate the instrument motion.

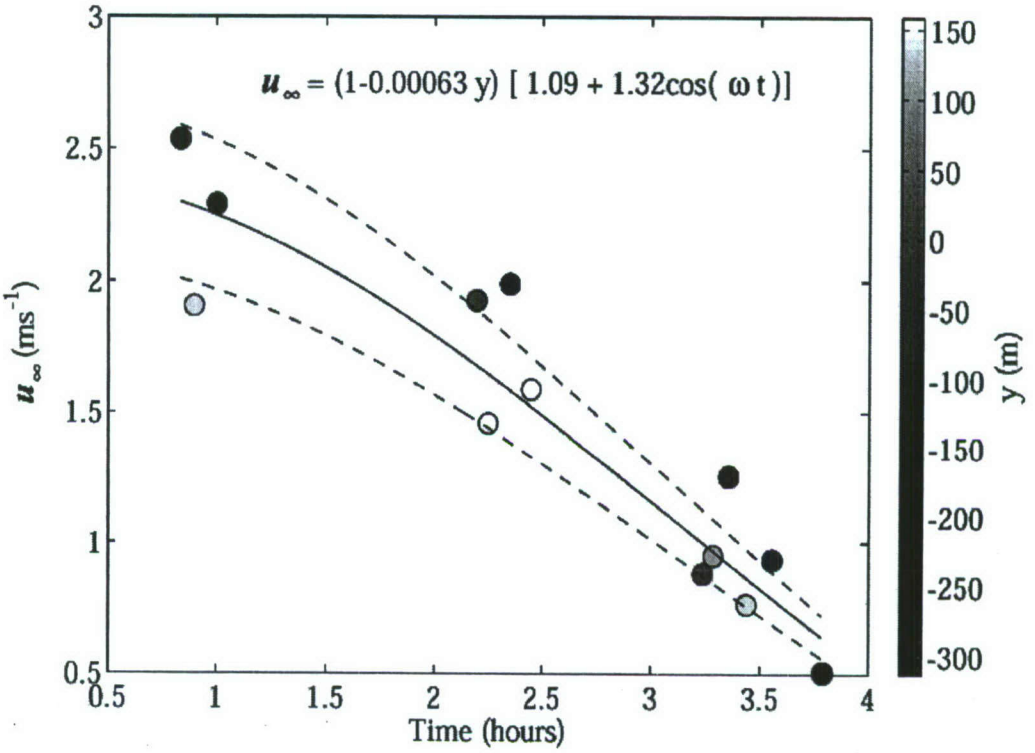

FIG. 2. Temporal and transverse variations of the free-stream velocity. Filled circles are averages of observed streamwise velocity outside of the turbulent wake. Grey shadings represent the transverse distance from the centerline of the wake. The solid curve is the fit of observations to a model current field consisting of a transverse shear, a mean current, and a semidiurnal tidal current. Dashed curves represent the 95% confidence interval of the model fit.

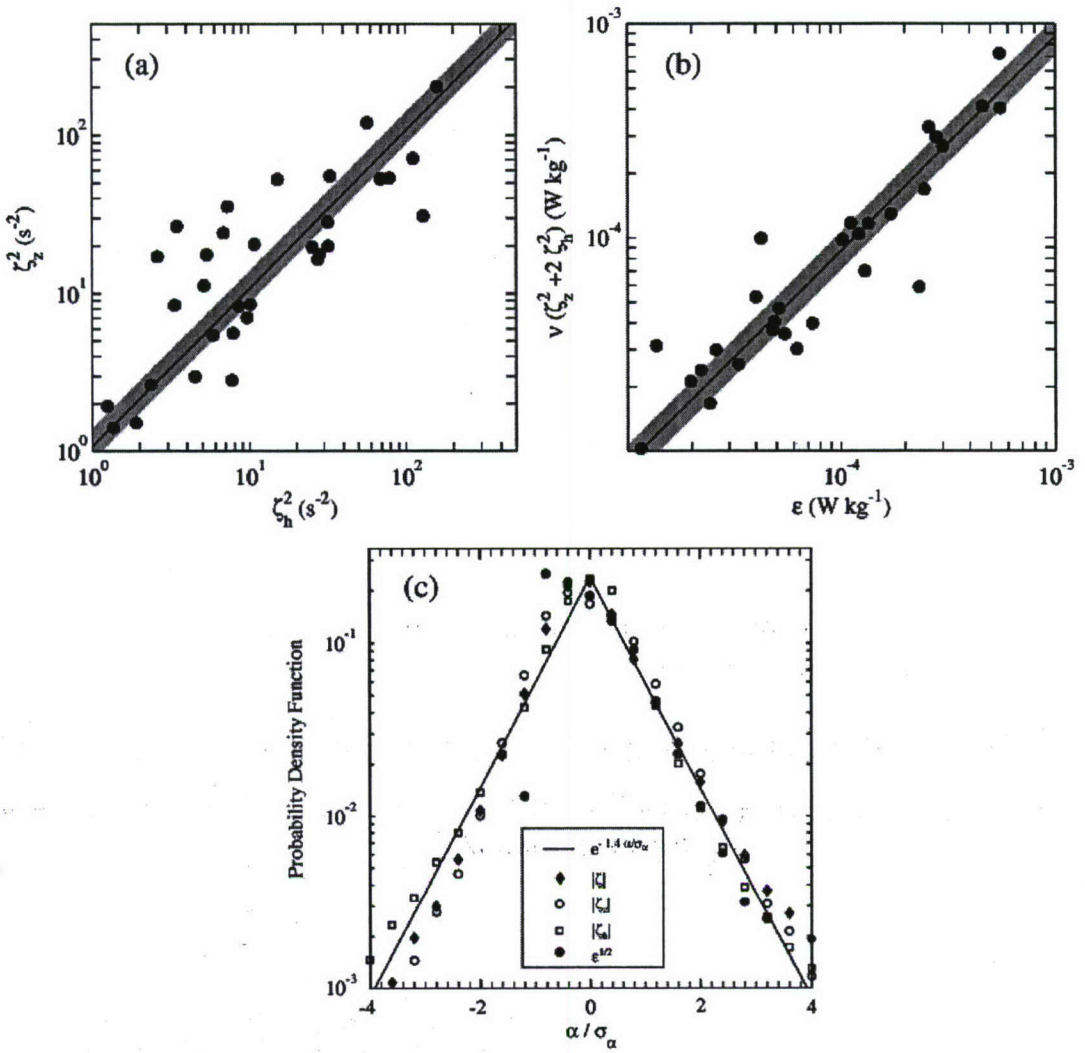

FIG. 3. (a) Comparison of the horizontal and vertical components of vorticity variances measured from the EMVM, (b) comparison of estimates of total enstrophy and turbulence kinetic energy dissipation rates, and (c) probability density functions of the normalized squared root of ε (solid dots), demeaned, normalized magnitudes of horizontal vorticity ζ_h (open circle), of vertical vorticity ζ_z (open square), and of total vorticity ζ (black diamond). The black curve is the empirical curve [4]. The variable α represents demeaned $\varepsilon^{1/2}$, $|\zeta_h|$, $|\zeta_z|$, and $|\zeta|$, and σ_α represents its standard deviation.

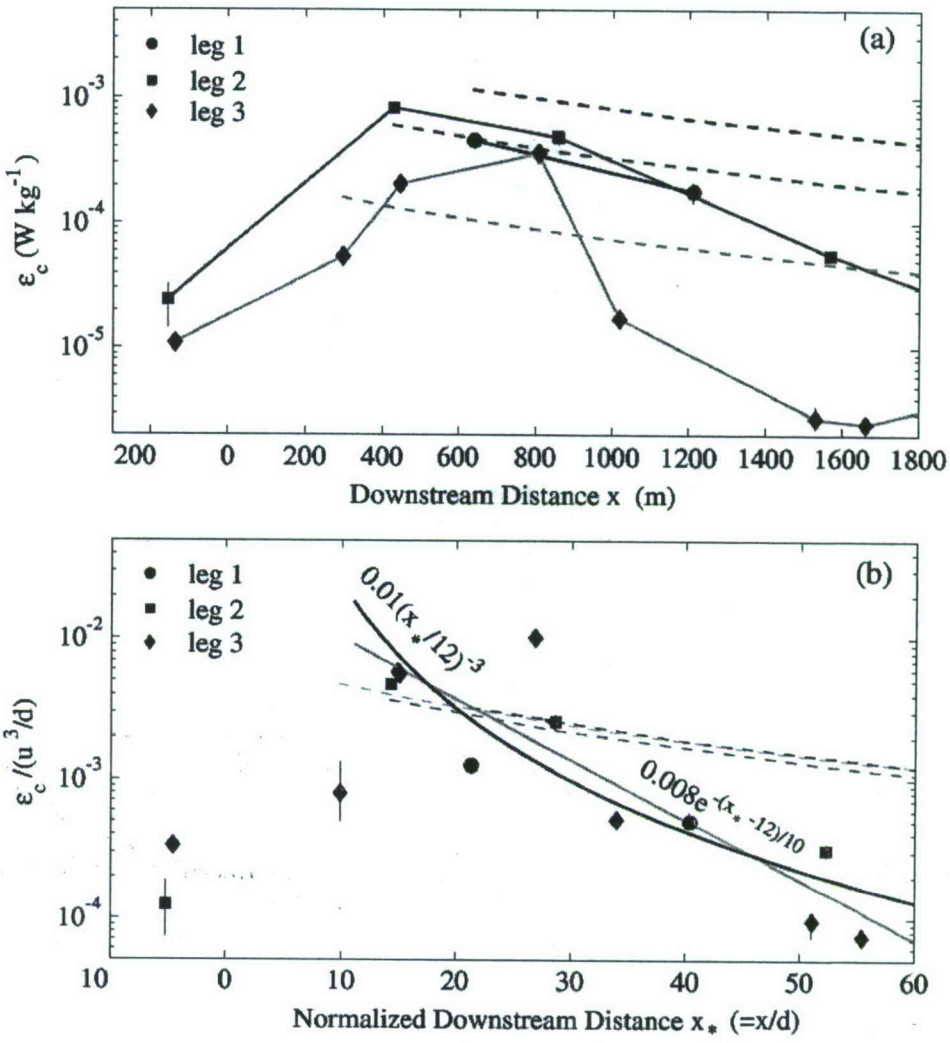

FIG. 4. (a) Downstream variation of turbulence kinetic energy dissipation rates along the centerline of the turbulent wake (solid lines with symbols), and (b) the non-dimensional form of (a) where the downstream distance is normalized by the scale of the pier d, and the turbulence kinetic energy dissipation rates normalized by u_∞^3 / d where u_∞ is the free-stream velocity. The black, dark grey, and light grey curves in (a) are model results for the three transects obtained by assuming the property of self-preservation similarity. The black and grey solid curves in (b) are power law fit and exponential law fit to observations.

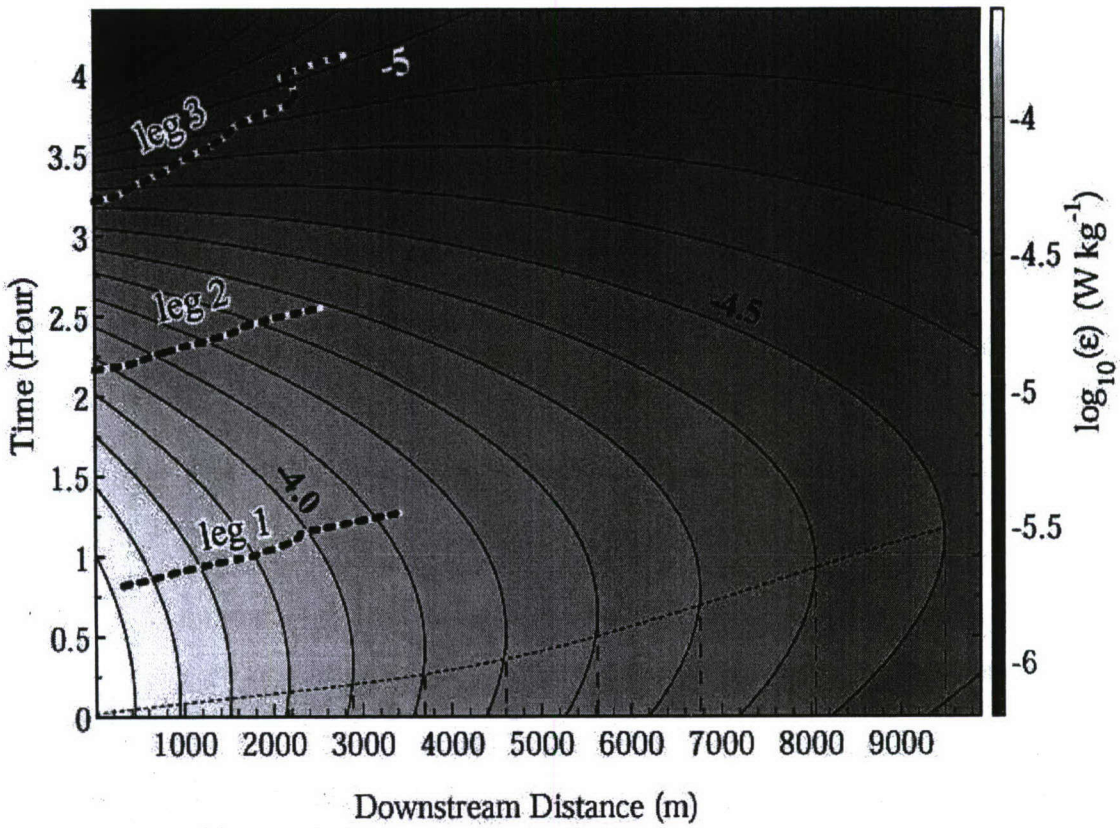

FIG. 5. Model spatial and temporal variations of ε induced by the ebbing tidal current interacting with the bridge pier. The tidal current model shown in Fig. 2 is used. Three thick dashed curves represent survey measurement tracks.

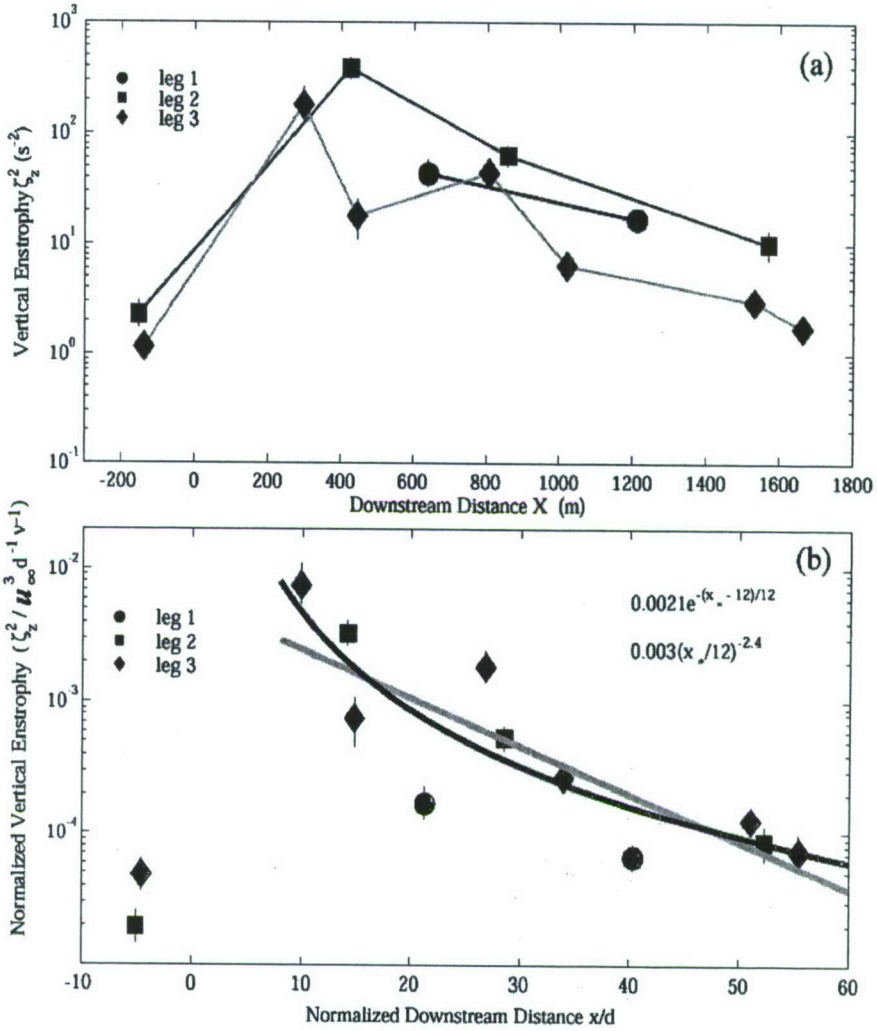

FIG. 6. (a) Downstream variation of the vertical component of enstrophy along the centerline of the turbulent wake (solid lines with symbols), and (b) the non-dimensional form of (a) where the downstream distance is normalized by the scale of the pier d and the enstrophy is normalized by $u_\infty^3 / d\upsilon$. The black and grey solid curves in (b) are the power law fit and the exponential law fit, respectively, to observations in $10 < x/d < 60$.

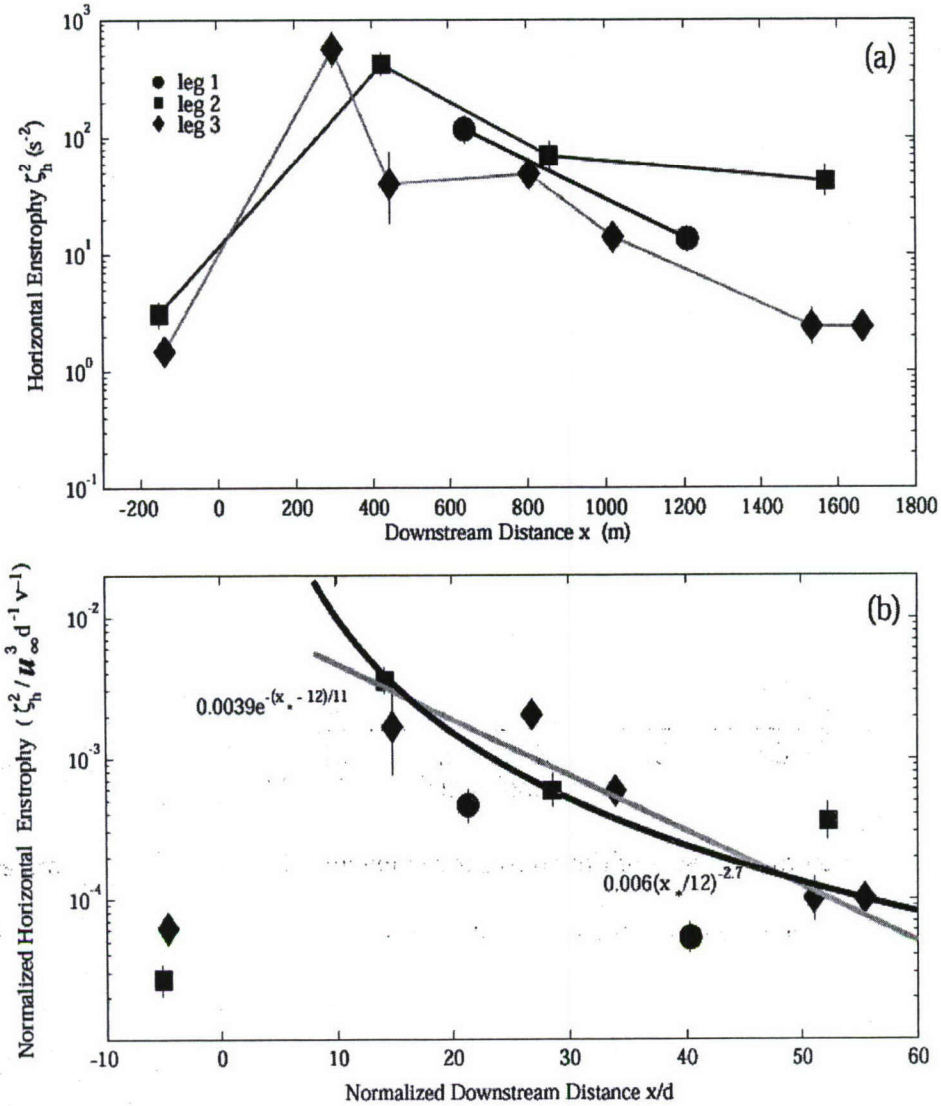

FIG. 7. (a) Downstream variation of the horizontal component of enstrophy along the centerline of the turbulent wake (solid lines with symbols), and (b) the non-dimensional form of (a) where the downstream distance is normalized by the scale of the pier d, and the enstrophy is normalized by $u_\infty^3 / d\upsilon$. The black and grey solid curves in (b) are the power law fit and the exponential law fit, respectively, to observations in $10 < x/d < 60$.

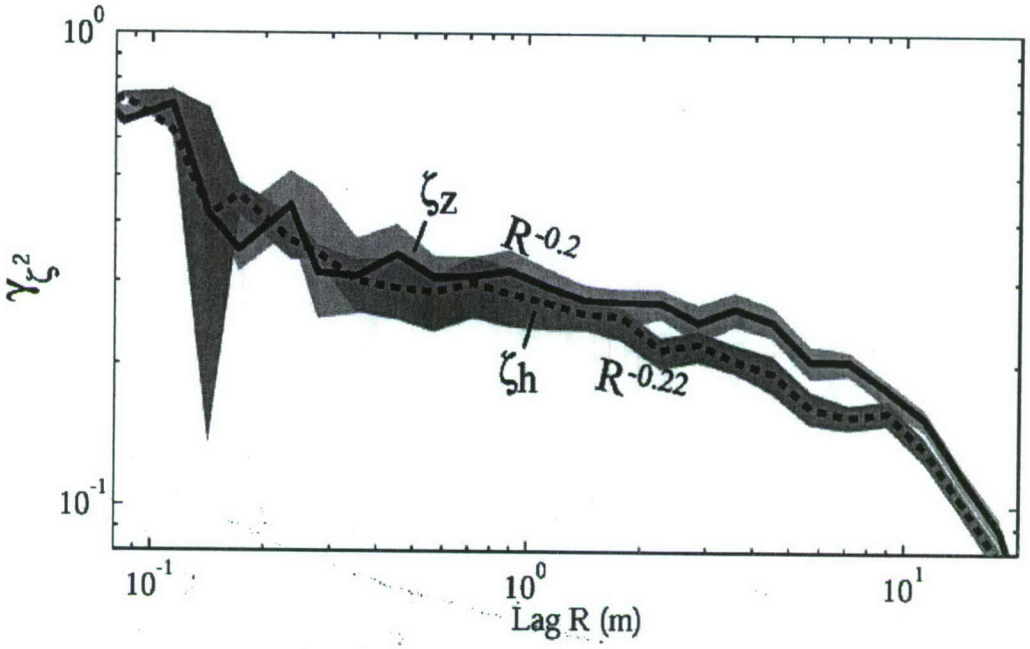

FIG. 8. Autocorrelation coefficients of vertical enstrophy ζ_z^2 (solid curve), and of horizontal enstrophy ζ_h^2 (dashed curve). Shadings are their 95% confidence intervals. The regression power-law fits in $0.3 < R < 4$ m, where R is the lag, are labeled.

Table 1. Measurements and sensors mounted on the Electro-Magnetic Vorticity Meter.

Measurement	Manufacturer	Sample rate (Hz)	Resolution
Vorticity (two)	APL-UW	20	3×10^{-4} s^{-1}
Velocity (two)	APL-UW	20	10^{-5} m s^{-1}
TKE dissipation	APL-UW	400	10^{-8} W kg^{-1}
Temperature	Sea-Bird	20	0.5×10^{-3} K
Conductivity	Sea-Bird	20	0.5×10^{-4} S m^{-1}
Pressure	Paroscientific	20	0.1 db
Magnetic heading	KVH, Inc.	1	0.1°
Pitch	IC sensors	20	0.035°
Roll	IC sensors	20	0.035°
Pitch rate	Humphrey	20	10^{-3}° s^{-1}
Yaw rate	Humphrey	20	10^{-3}° s^{-1}
Vessel Position	Northstar	0.5	3–5 m